Assessment of catchment response and calibration of a hydrological model using high-frequency discharge–nitrate concentration data

Rajesh R. Shrestha, Karsten Osenbrück and Michael Rode

ABSTRACT

This study uses a high-frequency discharge and nitrate concentration dataset from the Weida catchment in Germany for the catchment scale hydrologic response analysis. Nitrate transport in the catchment is mostly conservative as indicated by the nitrate stable isotope (δ^{15}N and δ^{18}O) analysis. Discharge–nitrate concentration data from the catchment show distinctive patterns, suggesting flushing and dilution response. A self-organizing feature map-based methodology was employed to identify such patterns or cluster in the datasets. Based on knowledge of the catchment conditions and prevailing understanding of discharge–nitrate concentration relationship, the clusters were characterized into five qualitative flow responses: (1) baseflow; (2) subsurface flow increase; (3) surface runoff increase; (4) surface runoff recession; and (5) subsurface flow decrease. Such qualitative flowpaths were used as soft data for a multi-objective calibration of a hydrological model (WaSiM-ETH). The calibration led to a reasonable simulation of overall discharge (Nash–Sutcliffe coefficient: 0.84) and qualitative flowpaths (76% agreement). A prerequisite for using such methodology is limited biogeochemical transformation of nitrate (such as denitrification).

Key words | cluster analysis, discharge–nitrate concentration relationship, hydrological flowpaths, model calibration, nitrate stable isotopes, self-organizing feature maps

Rajesh R. Shrestha (corresponding author)
Michael Rode
Department of Aquatic Ecosystem Analysis and Management,
UFZ – Helmholtz Centre for Environmental Research,
Brueckstrasse 3a, 39114 Magdeburg,
Germany
E-mail: rshresth@uvic.ca

Rajesh R. Shrestha
Pacific Climate Impacts Consortium,
PO Box 1700 STN CSC,
University of Victoria,
Victoria, British Columbia,
Canada V8W 2Y2

Karsten Osenbrück
Department of Isotope Hydrology,
UFZ – Helmholtz Centre for Environmental Research, Theodor-Lieser Str. 4, 06120 Halle,
Saale,
Germany
and
Water & Earth System Science (WESS),
University of Tuebingen,
Hölderlinstr. 12, 72074 Tübingen,
Germany

INTRODUCTION

Previous studies on temporal and spatial patterns of nutrient fluxes from catchments indicate that hydrological connectivity by subsurface flow is a key driver of nitrate mobilization and transport processes (Stieglitz *et al.* 2003; Ocampo *et al.* 2006a). Studies from different catchments (Creed *et al.* 1996; McHale *et al.* 2002; Ocampo *et al.* 2006b; Rusjan *et al.* 2008; Rode *et al.* 2009; Hesser *et al.* 2010) found evidence of strong linkage between hydrological flowpath and nitrate transport. Hence, hydrological flowpath could provide a basis for understanding the nitrate transport process. Furthermore, streamflow concentration and isotopic composition could yield insights into many key questions in catchment hydrology (Kendall & McDonnell 1998; Kirchner *et al.* 2004).

Similar to flushing of near-surface dissolved organic carbon by rising water table (Hornberger *et al.* 1994),

discharge and nitrate concentration datasets in many streams exhibit distinctive patterns. Characteristic nitrate concentration peaks preceding or succeeding the discharge hydrograph peaks followed by steady declines in the concentration have been observed in catchments of different sizes, such as: 135 ha Archer Creek catchment (Inamdar *et al.* 2004); 10.5 km^2 Turkey Lakes catchment (Creed & Band 1998); 42 km^2 Padež catchment (Rusjan *et al.* 2008); 46 km^2 River Dart catchment (Webb & Walling 1985); and 114 km^2 Zwalm catchment (Van Herpe & Troch 2000). In general, the early nitrate concentration peaks seem to be a characteristic of smaller catchments (e.g., Creed & Band 1998; Inamdar *et al.* 2004), which has been attributed to rapid flushing from near-surface soil layers or displacement of nitrate-rich till waters by infiltrating precipitation. The

lagged nitrate concentration peaks have been observed primarily in meso-scale catchments (e.g., Webb & Walling 1985; Van Herpe & Troch 2000; Rusjan *et al.* 2008), which has been attributed to delayed subsurface flow response from catchment uplands and/or saturated throughflow process, which gradually flush nitrate from enriched soil horizons.

Steady decline in nitrate concentration after the flushing response is another characteristic pattern of nitrate response. Van Herpe & Troch (2000) attributed the decline to diluting effect of surface runoff. In humid agricultural catchments, shifts from a 'flushing' or 'concentration' pattern in spring to a 'dilution' storm pattern in the fall and winter have been observed (Peter 1988; Vanni *et al.* 2001; Petry *et al.* 2002; Salvia-Castellvi *et al.* 2005; Poor & McDonnell 2007). Webb & Walling (1985) explained such shift in terms of flows from increased soil moisture and/or expanded saturation areas. Such conditions could lead to quickflow response during winter storms, and, as a consequence, marked dilution responses occur.

The cited studies indicate that nitrate 'flushing' and 'dilution' response could be prevalent in small to meso-scale catchments. The assumption could especially be valid in upland catchments with quick hydrological response (with soils and bedrock of low permeability, where regional groundwater flow is of minor importance; e.g., Soulsby *et al.* 2007; Hesser *et al.* 2010), where the fast groundwater flow quickly flushes out the accumulated nitrate from a catchment, and the quickflow from saturated areas provides the diluting influence.

Therefore, understanding such 'flushing' and 'dilution' processes in a catchment could provide insights into the mixing and transport of soluble nitrate from different hydrological flowpaths. Kirchner *et al.* (2004) argued that high-frequency measurements of chemical behavior could yield novel insights into many key questions in catchment hydrology. Conservative tracers are commonly used for such evaluation. However, most of these conservative tracers (e.g., Mg, Cl, Na, or environmental isotopes) can only be detected by chemical or isotope analyses and long-term high-frequency values are difficult to obtain. An alternative is to use the constituents like nitrate, which can be acquired at high-frequency resolution (such as hourly or sub-hourly) through optical sensor technology. However, given the

natural biogeochemical transformation (denitrification) of nitrate, it is necessary to analyze the transformation processes. In catchments with limited nitrate transformation, it may be possible to use the nitrate concentration data for characterizing the hydrological response.

The characterization of the hydrological flow response is especially relevant, given that it is poorly understood in most catchments. Although hydrograph separation methods such as digital filters (e.g., Arnold *et al.* 1995; Spongberg 2000; Eckhardt 2005) allow quantification of catchment response to storm events, they lack physical basis for explanation of the responses (Furey & Gupta 2001). On the other hand, flow components simulated by hydrological models are rarely calibrated, mainly due to the lack of information on subsurface flow. The hydrological models also suffer from the problem of equifinality (Beven & Freer 2001), as many different parameter sets within a chosen model structure can give similar model performances. In this context, hydro-chemical variables such as groundwater level and/or chemical concentration may provide supplementary information to constrain the model calibration within a plausible parameter set. Seibert & McDonnell (2002) provided an example of such an approach; they employed soft data (qualitative knowledge from catchment, e.g., new water ratio) in addition to hard data (runoff) for a multi-criteria calibration of a hydrological model. Their result indicated that the parameter set determined by multi-criteria calibration (using both hard and soft data) could better capture key processes controlling the catchment response. The case for multi-criteria calibration of hydrological models is also supported by other studies (e.g., Anderton *et al.* 2002; Bergström *et al.* 2002; Shrestha & Rode 2008), which indicated that the approach leads to a more plausible identification of model parameters and increased confidence of hydrological simulation. Therefore, the use of qualitative hydrological flow responses as soft data could also be a useful strategy for an improved hydrological model calibration.

This paper explores a methodology for characterizing patterns in discharge and nitrate-N concentration data and using the characterized patterns for calibration of a hydrological model. Prior to the use of nitrate concentration data for such characterization, nitrate stable isotope data were analyzed to verify basic assumptions on nitrate transport and

degradation processes. A self-organizing feature map (SOFM; Kohonen 1990; Kohonen et al. 1996) based methodology was employed for identification of patterns or clusters in the datasets. The clusters were characterized into qualitative flow responses based on the knowledge of catchment conditions and prevailing understanding of discharge–nitrate concentration relationship. The qualitative flow responses were employed as soft data for multi-objective calibration of a hydrological model (WaSiM-ETH). The study uses data from Weida catchment in north-eastern Germany, which is a sub-catchment of the Weisse Elster River in the Elbe River basin.

STUDY AREA AND DATA

The study area, the Weida catchment, covers an area of about 100 km^2 with relief varying from 357 to 552 m (Figure 1). Located in the lower mountain range in the state of Thuringia, Germany, the Weida stream is a small tributary of the Weisse Elster River in the Elbe River basin. The Weida stream flows into the Weisse Elster River through Zeulenroda reservoir, which is a part of the Thuringia drinking water supply system. Average annual precipitation in the catchment (1984–2003) is 630 mm, which is distributed throughout the year (March–May: 152 mm; June–August: 210 mm; September–November: 142 mm; December–February: 124 mm). Average mean temperature (1984–2003) in the catchment is 8.3 °C (March–May: 7.9 °C; June–August: 16.6 °C; September–November: 8.3 °C; December–February: 0.2 °C). Discharge at the Laewitz hydrometric station is perennial, with mean annual discharge of 0.6 m^3/s (March–May: 0.9 m^3/s; June–August: 0.3 m^3/s; September–November: 0.4 m^3/s; December–February: 1.0 m^3/s).

Geology of the catchment is dominated by clay shists and igneous rocks with low permeability. Soils developed from this bedrock range from shallow rankers to
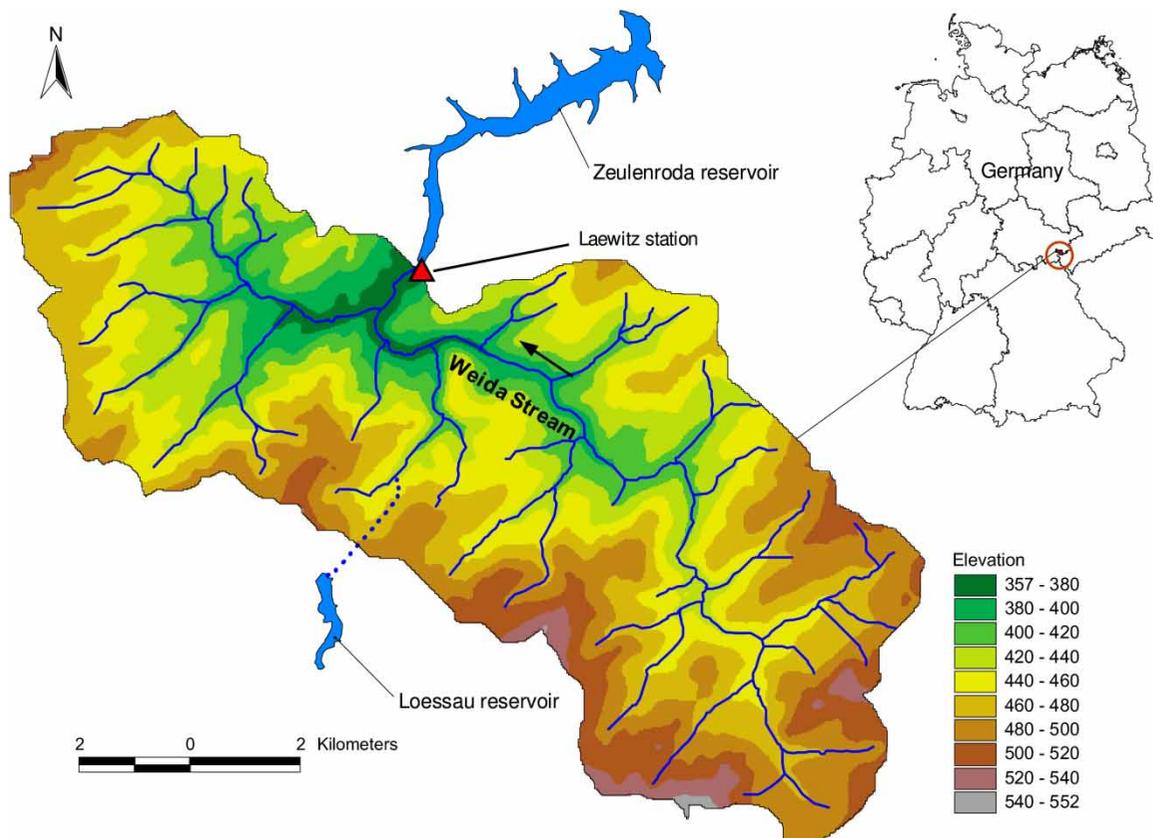

Figure 1 | Study area: Weida catchment.

well-developed cambisols and fluvisols in the stream valleys (Fink 2004). Sandy loam (40%) and silt loam (36%) are the dominant soil types in the catchment. Due to relatively low permeability, interflow appears to be the dominant runoff component in the catchment (Hesser *et al.* 2010). Land use in the catchment is dominated by arable land (40%), followed by forest (29%), and grassland (26%). Agricultural land use in the Weida catchment is moderately intensive. Arable crops are dominated by winter wheat, winter barley, rape, maize, sugar beet, and potato. Typical fertilizer application rates are 125 kg ha^{-1}yr^{-1} (winter wheat), 150 kg ha^{-1}yr^{-1} (maize), 70 kg ha^{-1}yr^{-1} (summer barley), and 90 kg ha^{-1}yr^{-1} (oats) (Fink 2004).

DATA AND ANALYSIS

Nitrate data and discharge–nitrate concentration relationship

Discharge and nitrate-N data at 1-minute intervals is available from the Laewitz monitoring station at the mouth of the Zeulenroda reservoir (Figure 1). The monitoring system employs a photometric sensor (Stamosens CNM750/CNS70, Endress + Hausser) with a maximum measurement error of 2% or ±0.1 mg L^{-1} in clear water condition (Hesser *et al.* 2010). The sensor uses a multiple beam flash process for continuous monitoring of nitrate concentration without chemical analysis. However, the nitrate-N concentration data obtained from the sensor are discontinuous due to missing values. In addition, the data consist of noticeable noise and errors.

For this study, three consistent winter–spring datasets from the years 2001, 2003–2004, and 2004 were selected (Table 1) and aggregated to an hourly time step. The three selected periods consist of the highest peaks and the highest nitrate-N concentration in the available datasets. Additionally, the three winter–spring high flow data were selected because nitrate-N concentration data during low flow summer conditions may be influenced by higher denitrification and biotic uptake. Mean temperature during the periods fluctuates between below freezing to above freezing, causing frequent snow accumulation and melt. Therefore, both precipitation and snowmelt contribute to the runoff.

Statistical characteristics of the discharge and nitrate-N concentration data used in this study are summarized in Table 1. Correlation coefficients between discharge and nitrate-N concentration are in between 0.34 and 0.54, implying some relation between the datasets. However, the magnitude and ranges of the three datasets are considerably different. For example, 2001 (2003–2004) dataset has the highest (lowest) mean discharge but the lowest (highest) mean nitrate-N concentration. Discharge–concentration plots of the three datasets (Figure 2) also illustrate the variability in these periods. Although the three periods show similar loops, equivalent nitrate-N concentration values for a given discharge are different for the three periods and also within each period. Such differences show that nitrate responses are highly variable for different runoff periods, which may be due to differences in catchment moisture condition, nitrate input, and storage in the catchment. However, the discharge nitrate-N concentration loops (Figure 2) are all characterized by the anti-clockwise hystereses with peak nitrate-N concentration following the discharge peak, and lower nitrate-N concentration on the rising limb of discharge hydrograph in comparison to the receding limb. Such patterns in discharge–nitrate concentration were also observed in the similarly sized meso-scale catchments (e.g.,

Table 1 | Statistical characteristics of discharge and nitrate-N conc. data, correlation is between discharge and nitrate-N concentration data for a given period

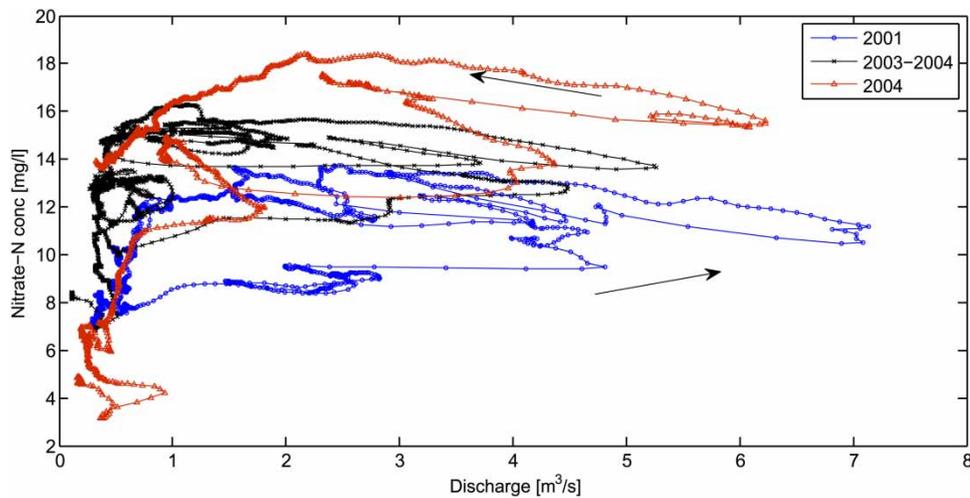| Year	Period	Data	Min.	Mean	Max.	Std. deviation	Corr. coef.
2001	March 1–May 1	Discharge [m^3/s]	0.29	1.51	7.13	1.35	0.52
		Nitrate-N conc. [mg/L]	7.08	10.02	13.75	2.02	
2003–04	Dec. 9–March 23	Discharge [m^3/s]	0.11	0.89	5.26	0.84	0.34
		Nitrate-N conc. [mg/L]	6.80	13.30	16.27	2.06	
2004	Oct. 28–Dec. 15	Discharge [m^3/s]	0.16	1.16	6.23	1.24	0.54
		Nitrate-N conc. [mg/L]	3.17	12.42	18.39	4.41	

Figure 2 │ Discharge–nitrate-N plots for three periods.

Webb & Walling 1985; Van Herpe & Troch 2000), where they explained the patterns in terms of 'concentration' and 'dilution' effects. Such patterns in the analyzed datasets also suggest prevalence of 'concentration' and 'dilution' effects in the Weida catchment, which could be used as a basis for characterizing hydrological flowpath as discussed in the Introduction.

The Weida stream also receives flow from the Loessau reservoir located outside the catchment (Figure 1) contributing about 10% of the total flow (Fink 2004). Since only weekly grab sample nitrate-N concentration data were available from the reservoir, direct characterization of the contribution of the external inflow to discharge–nitrate-N concentration relationship could not be undertaken. However, available data from the reservoir indicated that the average nitrate-N concentration (~5.0 mg/L) of the inflow was far less than the concentration in the Weida stream during the three periods of interest (Table 1). Therefore, the effect of mixing of low nitrate-N concentration external inflow could be assumed to be similar to the diluting effect of surface runoff.

Previous studies of nitrate transport in the Weida catchment (Shrestha *et al.* 2007; Hesser *et al.* 2010) indicated subsurface flow dominated transport. Results of the deterministic-fuzzy rule-based nitrate transport model by Shrestha *et al.* (2007) showed a strong relationship between subsurface flow and nitrate-N concentration. Results of the conceptual lateral nitrate transport model by Hesser *et al.*

(2010) indicated a dominant contribution of fast groundwater flow component, and a minor contribution of slow groundwater flow component. Computed mean residence time of groundwater flow was 22.5 months (2 months and 73.5 months for the fast and slow groundwater flow components, respectively, according to Hesser *et al.* (2010)). Due to such a short residence time, they suggested low denitrification in the dominant fast groundwater flow. Overall retention of nitrate leached from the unsaturated zone was computed to be 8%. Calculated total reduction capacity is lower than lowland catchments with glacial till or quaternary loess (Rode *et al.* 2009).

Nitrate fluxes from catchments may also be affected by the biotic uptake. High rates of nitrate transport typically occur during infrequent high flows whereas high rates of biological assimilation and storage typically occur during frequent low flows in streams (Royer *et al.* 2004), and rates of biological assimilation may be higher in the summer when temperature is warmer and biological activity is greater. At high nitrate loading rates, such as in the case of analyzed datasets, Mulholland *et al.* (2008) suggested that removal of N becomes ineffective and the stream network exports virtually all catchment-driven nitrogen. Similarly, Alexander *et al.* (2009) showed that for an agricultural stream (Indiana) with comparable high nitrate concentrations, N removal was nearly negligible from late autumn to the beginning of summer. Such observation is also supported by earlier studies (e.g., Hill 1979) which concluded

that during critical times of the year (i.e., high discharge, high NO_3–N concentrations) the export of NO_3–N from agricultural streams was not affected by biotic uptake and denitrification. Therefore, based on the results of such previous studies, the biotic uptake of nitrate can be reasonably assumed to be limited for the three high flow periods analyzed in this study.

Nitrate stable isotope sampling and analysis

In addition to continuous discharge and nitrate-N data, nitrate stable isotope ($\delta^{15}N$ and $\delta^{18}O$) data and concurrent major ions were obtained at the monitoring station at Laewitz from 2007 to 2009. The data were obtained from the analysis of a total of 115 grab samples taken at weekly intervals. At baseflow condition (28 May 2008), 14 supplementary stream samples were taken along the profile of the Weida stream and its major tributaries. Although the majority of the stream samples were taken during baseflow or hydrograph recession, most of the cold season samples represent water and nitrate fluxes near peakflow condition. Samples were filled in 0.5-L high-density polyethylene (HDPE) bottles and stored under cool conditions prior to measurement. Isotopes of nitrogen and oxygen of nitrate were analyzed using the denitrifier method (Sigman *et al.* 2001; Casciotti *et al.* 2002). The method uses gaseous N_2O, which is produced under controlled conditions from microbial degradation of nitrate dissolved in the water sample (for details see Shomar *et al.* 2008; Knöller *et al.* 2011). For the measurement of the isotopic composition of the produced N_2O, a modified gasbench II-system connected to a mass spectrometer delta V plus (Thermo) was used. Results are given as $\delta^{15}N$ and $\delta^{18}O$ values relative to the international references AIR and VSMOW (Vienna Standard Mean Ocean Water), respectively. The analytical uncertainties are in the range of $\pm 0.3‰$ for $\delta^{15}N$ and $\pm 1.0‰$ for $\delta^{18}O$.

The stable isotope nitrate data ($\delta^{15}N$ and $\delta^{18}O$) in stream water was analyzed to provide information on the source and transport process of nitrate in the Weida catchment. Of particular interest in this analysis is the extent of non–conservative processes like microbial denitrification. The results of the isotope analyses (Figure 3) indicate that the $\delta^{15}N$ and $\delta^{18}O$ values of most samples fall in a range that

is common for nitrate in watersheds with dominant agricultural land use (Kendall & Aravena 2000; Xue *et al.* 2009). The spreads of $\delta^{15}N$ and $\delta^{18}O$ values are small during the sampling period of more than 2 yr. This suggests that most of the nitrate in stream water originates from a few dominating sources including NH_4-fertilizer and manure applications. Buda & DeWalle (2009) reported similar findings in watersheds dominated by agricultural land use, which also included storm events. Persistently low $\delta^{18}O$ nitrate values ($<+7‰$, see Figure 3) including high flow condition indicate that nitrate from atmospheric deposition or NO_3-fertilizer application (both usually characterized by $\delta^{18}O$ values greater than $+15‰$ according to Xue *et al.* (2009) and Kendall & Aravena (2000)) are of minor importance or not directly (i.e., via transformation to reduced N compounds) released to the hydrological flowpaths. A few stream samples with higher $\delta^{15}N$ values are probably due to the increased influence of effluents from sewage treatment plants or septic tanks along the Weida stream during baseflow conditions.

Unlike conservative tracers, the transport of nitrate in subsurface flow may additionally be affected by biogeochemical processes like microbial denitrification. If denitrification takes place, the $\delta^{15}N$ as well as $\delta^{18}O$ values of the residual nitrate are expected to become progressively enriched with

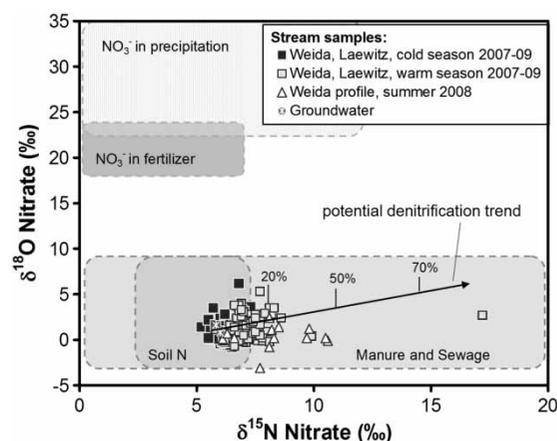**Figure 3** | $\delta^{15}N$ and $\delta^{18}O$ of nitrate in stream water of the Weida. Given for comparison are approximate ranges (gray boxes) for the isotopic composition of different sources of nitrate compiled from the literature (adapted from Kendall & Aravena (2000)). The direction of a possible isotope fractionation trend due to denitrification is indicated by the arrow. Numbers indicate the approximate fraction of nitrate removed by denitrification assuming an initial $\delta^{15}N$ value of $+6.2‰$ and an enrichment factor of about $-7‰$ (see text for details).

decreasing nitrate concentrations due to higher reaction rates of lighter isotopes (Kendall & Aravena 2000). According to Figures 3 and 4, there is no clear trend towards heavier isotopic composition (i.e., higher δ values) along the indicated lines. Mixing processes may reduce the magnitude of observed isotope enrichments if differences in the level of denitrification and hence in nitrate concentration and isotopic signatures of the mixing components are high (Green *et al.* 2010). In the Weida catchment, however, such differences between stream water and inflowing surface or groundwater are likely to be small. This is supported by homogeneous nitrate concentrations and isotopic signatures along a profile of the Weida River during baseflow conditions, as well as groundwater samples (Figures 3 and 4). Therefore, the low variability of nitrate stable isotopes suggests that nitrate released to and transported in the stream has not significantly been affected by denitrification in the subsurface or the stream itself during the investigated period. However, a small difference (about 1‰) between the isotopic composition of stream nitrate during the warm and cold seasons (higher mean $\delta^{15}N$ value in summer as compared to a lower mean in the

winter and fall seasons, see Figure 3) was observed. This indicates that denitrification cannot be ruled out completely, although seasonal variations in isotopic compositions may also be due to variations in the dominating N sources (Savard *et al.* 2010). A conservative estimate of the maximum amount of denitrification may be obtained by making the unlikely assumption that the spread of data in the direction of the trend line in Figure 3 is mainly due to denitrification. For the calculation, the difference of the 80th and 20th percentiles of the observed $\delta^{15}N$ values was used as a measure of the isotope enrichment during a Rayleigh-type process with an enrichment factor of -5 to $-7‰$, which is in the lower range of values reported in the literature from natural, not diffusion controlled water systems (Mariotti *et al.* 1981; Sebilo *et al.* 2003). The calculation shows that a maximum of 20% of nitrate, but most probably less, has been removed from solution by denitrification processes. A low denitrification is also in correspondence with the slight increase of $\delta^{15}N$ values with decreasing nitrate concentrations in Figure 4(b). However, most probably a large part of the trend in Figure 4(b) is due to mixing of different sources of nitrate that may be expected from the different water flow-paths contributing to stream runoff during storm and baseflow conditions. Due to only small variations of isotope values, mixing of different N sources and a small contribution from denitrification cannot be separated. If minor denitrification is present in the catchment, it is associated with low discharge conditions as indicated by an increased mean $\delta^{15}N$ value during low discharge conditions in Figure 4(a). Therefore, the results of nitrate stable isotope analyses suggest that the transport of nitrate in the Weida catchment can be reasonably well described by conservative transport processes, i.e., by advection along hydrological flowpaths. This is particularly the case during high discharge conditions, when low values of nitrate stable isotopes provide no evidence of the presence of denitrification.

In summary, nitrate transport and transformation processes in the Weida catchment during high flow conditions can be considered to be dominated by fast groundwater flow and interflow-driven processes, and limited residence time (according to Hesser *et al.* (2010)). In addition, under such high flow conditions, nitrate fluxes can be reasonably considered to be affected by limited denitrification (based on the stable isotope analysis) and biotic uptake. Such
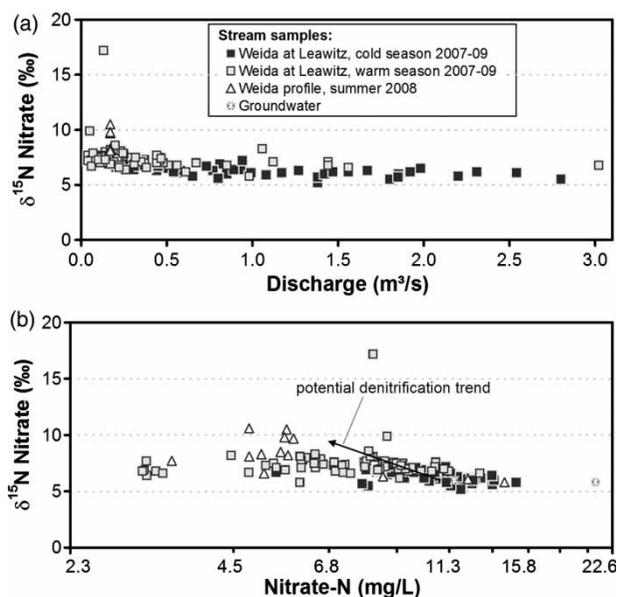

Figure 4 │ Relationship between $\delta^{15}N$ of nitrate and (a) discharge of the Weida at Laewitz and (b) nitrate-N concentration in stream water of the Weida at Laewitz. Note the log scaling of nitrate-N concentrations. The arrow indicates the direction of a possible isotope fractionation trend for denitrification in natural water fluxes (Mariotti *et al.* 1981; Sebilo *et al.* 2003).

characteristics provide a reasonable basis for employing nitrate for the hydrological flowpath analysis.

MODELING APPROACH

Cluster analysis of discharge–nitrate concentration data

This study used a SOFM (Kohonen 1990; Kohonen *et al.* 1996) based methodology for identification of clusters in discharge–nitrate concentration data. The SOFM is a type of artificial neural network, which learns to classify input vectors by mapping patterns in datasets. It converts complex, nonlinear statistical relationships (in a high-dimensional space) into simple relationships (in a low-dimensional space) based on regularities and correlations in the datasets. As it compresses information while preserving the important topological and metric relationships, it can be described as a model for knowledge abstraction (Kohonen *et al.* 1996). The abstraction of information in a SOFM from high-dimensional data to low-dimensional output takes place in an unsupervised manner.

A wide range of applications of the SOFMs in hydrology have been reported in the recent literature, such as characterization and diagnosis of groundwater quality (Hong & Rosen 2001), decomposition of effective rainfall runoff data into different segments (Jain & Srinivasulu 2006), estimation of design hyetographs of ungauged sites (Lin & Wu 2007), and classification of sediment quality (Alvarez-Guerra *et al.* 2008). A review of applications of SOFMs in hydrology is available in the ASCE Task Committee on application of Artificial Neural Networks in Hydrology (2000a, b) and Kalteh *et al.* (2008). More details on the SOFM are available in Kohonen (2001) and Kohonen *et al.* (1996).

The SOFM models were developed using an algorithm found in the MATLAB Neural Network Toolbox (Demuth *et al.* 2009). The first step in SOFM-based discharge–nitrate-N concentration cluster identification is the selection of appropriate input variables. With the selected input variables, the SOFM should be able to identify all relevant patterns in discharge and nitrate-N concentration data, such as changes in nitrate-N concentration corresponding to discharge. Preliminary SOFM trainings with discharge and nitrate-N concentration time series as inputs only led to a division of the two input datasets into clusters of different ranges and could not capture rising and falling patterns in the datasets. Therefore, besides discharge (Q) and nitrate-N concentration (N) data series, a rate of change of these variables (dQ/dt and dN/dt) were employed as additional inputs. These inputs provide information on the rising and falling pattern datasets and could guide the SOFM training to distinguish such changes. Therefore, the SOFM cluster QN_{cluster} can be expressed as a function of these four input variables:

$$QN_{\text{cluster}} = f(Q, N, dQ/dt, dN/dt) \tag{1}$$

Since the four input datasets are of different ranges, it is important to normalize the input datasets so that the dataset with a higher variability does not dominate SOFM training. For this reason, all four input vectors were normalized to zero mean and one standard deviation. Additionally, discharge and nitrate-N concentration data were weighted by 2 (by trials), so that minor changes in dQ/dt and dN/dt do not affect the cluster identification process.

After the definition of input vectors, an appropriate architecture of the SOFM needs to be designed. Since a large network may lead to overfitting (Alvarez-Guerra *et al.* 2008), SOFM training should be started with a small number of neurons and gradually increased to achieve satisfactory output. In the present application, the SOFM training was started with 3×2 neurons, and SOFM architecture with a 4×3 neurons was found to be adequate to capture the rise and fall of discharge and nitrate-N concentration at different data ranges. Initially, the SOFM trained with the 2003–2004 dataset was used for the simulation of 2001 and 2004 clusters. However, the simulated clusters were not able to represent the relationships in these datasets. As outlined previously, each of the 2001, 2003–2004, and 2004 datasets have different variability with different ranges of discharge and nitrate-N concentration datasets related to one another. Therefore, the SOFMs were trained for individual datasets. Since the cluster results are to be later used for the hydrological model calibration and meteorological inputs required for the hydrological model are available only at a daily resolution (explained later), the SOFMs were also retrained for a daily time step.

The characterization of the cluster results was supported by the prevailing knowledge on the catchment scale hydrological and nutrient response (such as the 'concentration' and 'dilution' effects), and understanding of the flow–nitrate transport relationship in the Weida catchment. Although the cluster results were not sufficient to quantitatively separate the flow into surface runoff and subsurface flow components, qualitative responses could be defined based on the dynamics of discharge and nitrate concentration response.

Hydrological model setup and calibration

The qualitative hydrological flow responses defined from discharge and nitrate-N clusters were used for calibration of flow components simulated by the Water balance Simulation Model, WaSiM-ETH (Schulla 1997; Schulla & Jasper 2007). The WaSiM-ETH was chosen for this catchment as it has been successfully applied for similar mountainous catchments in the region (Rode & Lindenschmidt 2001; Lindenschmidt et al. 2004; Shrestha & Rode 2008).

WaSiM-ETH is a process-based distributed modeling system capable of simulating different hydrological processes at different spatial and temporal scales. The model can simulate catchment response, as well as hydrological flow components. The WaSiM-ETH uses a modular, object-oriented architecture for simulation of different hydrological processes such as evapotranspiration, snow accumulation, snow melt, infiltration and generation of surface and subsurface flow components. WaSiM-ETH uses the Green and Ampt/TOPMODEL approach for runoff generation and soil water balance simulation. The Green and Ampt equation calculates infiltration based on soil moisture condition, and surface runoff occurs when infiltration exceeds soil infiltration capacity. WaSiM-ETH implementation of TOPMODEL (Beven & Kirkby 1979) simulates soil water balance and runoff generation separately for each grid cell based on the spatial distribution of soil topographic index. The model generates surface runoff when unsaturated zone is filled, which is routed in streams using a kinematic wave approach. More information on the model is available in Schulla & Jasper (2007).

The WaSiM-ETH hydrological model was set up for the Weida at a 100-m grid resolution using: (1) a digital elevation model from Thüringen State Land Surveying Office (2003); (2) land use data based on the 1999 Landsat-ETM image classification (Bongartz 2004); and (3) soil data based on 1:25,000 soil map with supplementary classification based on local soil profiles (Fink 2004). The model was run at a daily time step since the daily meteorological inputs (i.e., precipitation, temperature, global radiation, relative sunshine duration, wind velocity, relative humidity, and vapor pressure) were available. Due to this limitation, subdaily variations of the catchment hydrological response and their relation with nitrate concentration could not be analyzed. Precipitation data from five stations and meteorological data from three nearby stations were used. Spatial interpolation of the forcing data were carried out using an inverse distance weighting algorithm. Discharge from Loessau reservoir was introduced as external inflow.

An indirect methodology was formulated to employ discharge–nitrate-N cluster results (as soft data) for calibration of simulated flow components. The methodology uses a number of rules to compare characteristics of WaSiM-ETH simulated hydrological flow components (such as whether surface runoff or subsurface runoff is increasing or decreasing) with the cluster classes. An example of the rule for cluster agreement (clust_agree) calculation is given below:

$$
\begin{aligned}
&\left.\begin{array}{l} \text{if } Q_{sub}(t+1) > Q_{sub}(t) \\ \quad \& \text{clust} = 2 \end{array}\right\} \text{clust\_agree} = 1 \\
&\text{else clust\_agree} = 0
\end{aligned}
\tag{2}
$$

where $Q_{sub}(t)$ is subsurface flow at time step t and clust is a cluster class.

Similarly, cluster agreements for each time step and for all clusters were calculated. The objective function (obj$_1$) for the multi-objective calibration of WaSiM-ETH was formulated as a weighted sum of cluster agreements (clust_agree):

$$
\text{obj}_1 = \text{agree} = -\frac{\sum_{j=1}^{n} \text{clust\_agree}}{n}
\tag{3}
$$

The second objective function, the Nash–Sutcliffe coefficient of efficiency (NSCE) was employed to evaluate the

'goodness of fit' of total runoff simulation:

$$\text{obj}_2 = 1 - \text{NSCE} = \frac{\sum\limits_{j=1}^{n} \left(Q_{j,\text{obs}} - Q_{j,\text{sim}} \right)^2}{\sum\limits_{j=1}^{n} \left(Q_{j,\text{obs}} - \overline{Q}_{\text{obs}} \right)^2} \quad (4)$$

where n is number of observations, $Q_{j,\text{obs}}$ and $Q_{j,\text{sim}}$ are observed and simulated discharges at time step j, and $\overline{Q}_{\text{obs}}$ is mean observed discharge. 1-NSCE and negative of the agree values were used to express the objective functions for minimization. Two additional criteria, coefficient of determination (R^2) and mean absolute error (MAE) were used for further evaluation of model performance.

The model calibration was performed by adjusting nine model parameters that affect the runoff generation processes. These parameters are highly interdependent and together affect the contribution of different flow components to the total flow (Schulla & Jasper 2007). Parameter ranges for calibration were defined from calibrated models in similar catchments (Shrestha *et al.* 2007; Shrestha & Rode 2008), which are summarized in Table 2. The 2003–2004 and 2001 period data were employed for model calibration and validation, respectively. A warm-up period of 1 yr was used. The multi-objective optimization tool called the non-dominated sorting genetic algorithm-II (NSGA-II; Deb *et al.* 2002) was used to evaluate the performance of two objective functions. The NSGA-II is a fast and elitist multi-objective genetic algorithm capable of finding multiple Pareto solutions in a single optimization run. Key features of the NSGA-II are an efficient sorting algorithm and maintenance of a diverse set of elite population. More details on the NSGA-II algorithm are available in the original work by Deb *et al.* (2002), which is also summarized in Shrestha & Rode (2008). Ten independent optimization runs of NSGA-II were carried out with a population size between 100 and 130 and the number of generations between 25 and 30, based on which preferred solution was selected.

RESULTS AND DISCUSSION

Cluster analysis of discharge and nitrate-N data

SOFMs trained with the two-dimensional 4×3 neurons produced 12 clusters of discharge–nitrate-N concentration time series data. The 12 clusters captured five different patterns or relationships in the data series with a number of clusters capturing the same patterns at different data ranges. These patterns consist of: (1) constant discharge and/or nitrate-N concentration or small change: $\{Q(t+1) \approx Q(t), N(t+1) \approx N(t)\}$; (2) increase in discharge and nitrate-N concentration: $\{Q(t+1) > Q(t), N(t+1) > N(t)\}$; (3) increase in discharge and decrease in nitrate-N concentration: $\{Q(t+1) > Q(t), N(t+1) < N(t)\}$; (4) decrease in discharge and increase in nitrate-N concentration: $\{Q(t+1) < Q(t), N(t+1) > N(t)\}$;

Table 2 │ Description, minimum, maximum and optimal values of the parameters used in the WaSiM-ETH calibration. Units are given in parentheses

Parameter	Description	Min.	Max.	Optimal parameter
m	Recession parameter for base flow [m]	0.001	0.1	0.0076
T_{cor}	Correction factor for transmissivity of soil [–]	0.00001	0.001	0.00081
K_{cor}	Correction factor for vertical percolation [–]	1	50	13.8
k_D	Single reservoir recession constant for surface runoff [h]	1	80	44.7
SH_{max}	Maximum storage capacity of interflow storage [mm]	10	50	33.6
k_H	Single reservoir recession constant for interflow [h]	30	250	244.8
P_{thres}	Precipitation intensity threshold for generating preferential flow into saturated zone [mm day^{-1}]	0.01	10	4.3
r_k	Scaling factor for capillary rise/refilling of soil storage from interflow [–]	0.1	1	0.99
c_{melt}	Fraction of snowmelt which is surface runoff [–]	0.016	1	0.37

and (5) decrease in discharge and nitrate-N concentration: $\{Q(t+1) < Q(t),\ N(t+1) < N(t)\}$. Accordingly, the 12 clusters were reclassified into five classes to represent such distinct flow responses. The reclassified clusters for the 2001, 2003–2004, and 2004 periods are shown in Figures 5(a), 5(b), and 5(c), respectively. The five identified cluster classes were conceptually characterized into water and solute contributions from different flowpaths. Previous studies on 'flushing hypothesis' (Creed *et al.* 1996) and 'concentration' and 'dilution' effects (Webb & Walling 1985; Peter 1988) together with the results of previous studies of the Weida catchment (Shrestha *et al.* 2007; Hesser *et al.* 2010) were used as a basis for characterization, which are described below.

Cluster (1) $\{Q(t+1) \approx Q(t),\ N(t+1) \approx N(t)\}$: This cluster is characterized by low flow and low nitrate-N concentration, and/or small changes between two time steps. The region has nitrate-N concentration between 4.1 and 8.6 mg/L, which according to the previous study of the Weida catchment (Hesser *et al.* 2010) corresponds to slow groundwater flow or baseflow (with mean residence time 73.5 months) region. The evaluation of soil moisture during the analysis periods showed high saturation deficit, similar to the stage 1 (baseflow) in Creed *et al.* (1996). Based on such observations, the cluster is conceptualized as the baseflow region.

Cluster (2) $\{Q(t+1) > Q(t),\ N(t+1) > N(t)\}$: This cluster includes the early portion of the rising limb of the discharge hydrograph, when nitrate-N concentration exhibits a steep increase. Analysis of the moisture conditions revealed declining soil saturation deficit. Such response is similar to stage 2: saturated subsurface flow as defined by Creed *et al.* (1996). In the Weida catchment, the model results by Hesser *et al.* (2010) indicate that interflow and fast groundwater flow components dominate nitrate transport. Since the fast groundwater flow component has a short residence time (2 months, according to Hesser *et al.* (2010)) and denitrification rate is low (according to stable isotope analysis), the rapid increase in nitrate-N concentration could be attributed to interflow and fast groundwater flow components. Since the cluster result is not sufficient to distinguish different components of the groundwater flow, the cluster is conceptualized as the sub-surface flow increase region.

Cluster (3) $\{Q(t+1) > Q(t),\ N(t+1) < N(t)\}$: This cluster includes the latter portion of the rising limb of the discharge hydrograph, when nitrate-N concentration declines. Previous analysis of the Weida catchment condition indicated decline of the nitrate-N concentration in the presence of surface runoff (Shrestha *et al.* 2007). Such dilution effect is typical in wet soil conditions especially during winter (Webb & Walling 1985) and could be attributed to the surface runoff. Dilution of nitrate by surface water has also been observed during intense rainfall events, where a considerable share of Horton excess surface runoff contributed to total discharge (Peter 1988). In this particular case, the decline of nitrate concentration in some cases also coincided with increased external inflow. These analyses indicate the influence of saturation excess surface runoff and/or external inflow from Loesau reservoir to the streamflow. Based on such observations, the decline in nitrate-N concentration in the stream can be considered as the diluting effect of nitrate poor surface runoff/external inflow mixes, and the cluster is conceptualized as the surface runoff increase region.

Cluster (4) $\{Q(t+1) < Q(t),\ N(t+1) > N(t)\}$: The cluster consists of the falling limb of the discharge hydrograph, when nitrate concentration increases. The increase in nitrate-N concentration may be due to rapid recession of saturated surface runoff with shrinking of saturated areas within the catchment and/or in this particular case, recession of external inflow from Loesau reservoir. Such conditions could cause nitrate-N concentration to increase as the diluting effect by nitrate poor surface runoff water is diminished, and the contribution of catchment uplands continue to sustain high nitrate concentration. Such patterns were also observed by Webb & Walling (1985) and Van Herpe & Troch (2000) in very sharp chemograph response due to rapid decline of discharge. Based on such characteristics, the cluster is conceptualized as the surface runoff recession region.

Cluster (5) $\{Q(t+1) < Q(t),\ N(t+1) < N(t)\}$: The decline in discharge and nitrate-N concentration in this cluster corresponds to flow recession. In such conditions, the contribution of nitrate-rich interflow and fast groundwater flow continues to decline. It is well known that with a further decrease in discharge, the proportion of the contribution of deeper groundwater increases and nitrate-N
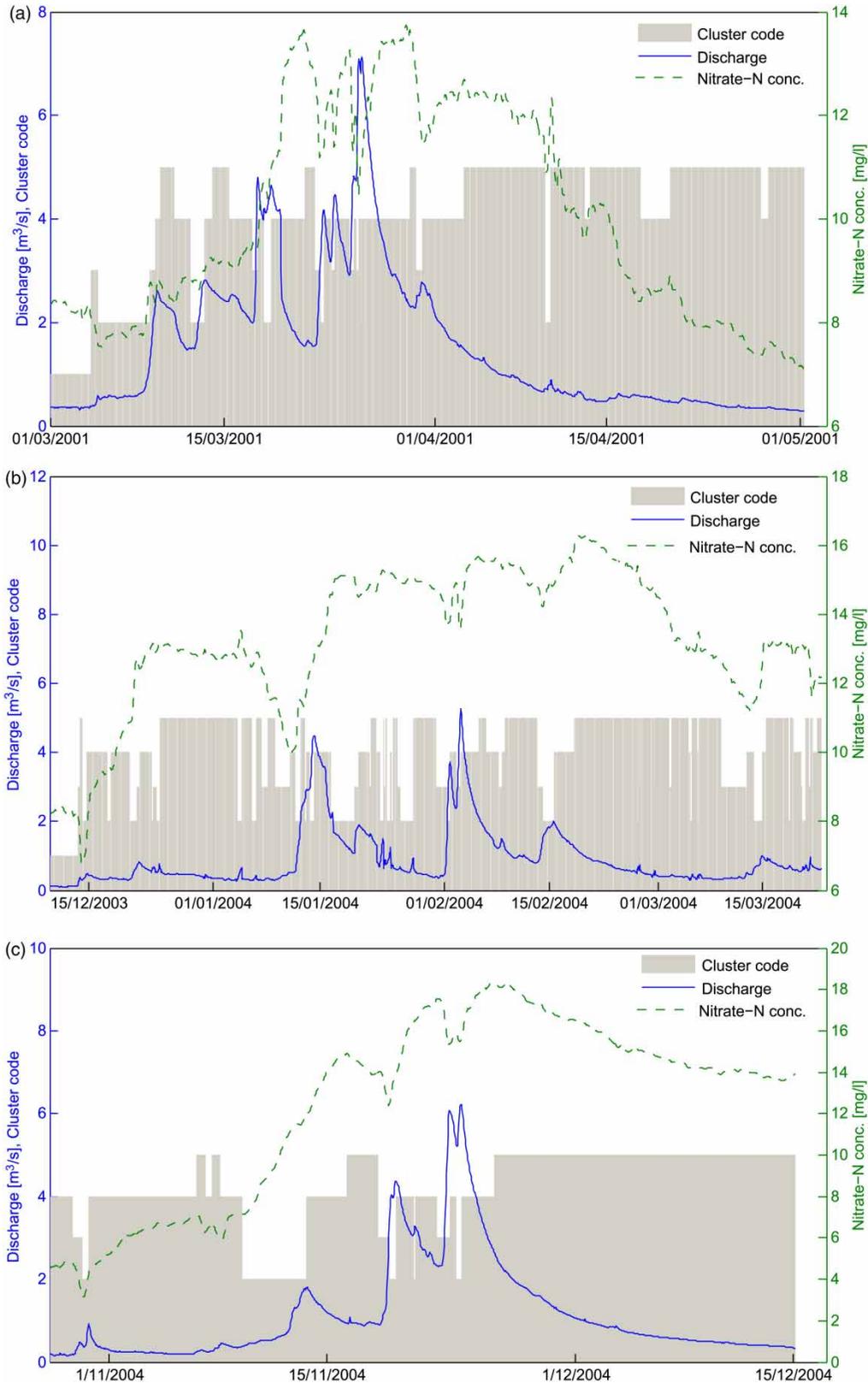
Figure 5 │ Results of SOFM after reclassification into five clusters for: (a) 2001 period; (b) 2003–2004 period; and (c) 2005 period.

concentration declines towards background groundwater concentration. Therefore, the region is conceptualized as the subsurface flow recession region.

The conceptual characterization of clusters provides qualitative representation of temporal dynamics of the discharge–nitrate relationship. Based on such characteristics, cluster classes, relative contributions of different flow responses to the total runoff, and nitrate concentration could be identified. Although the lack of nitrate concentration and discharge measurement data inside the catchment constrained a more objective characterization of flow response, the qualitative characterization based on cluster classification can be considered as a representation of dominant catchment-scale processes.

Model calibration using cluster results

The multi-objective calibration of the WaSiM-ETH model with cluster results as the soft data led to trade-offs between the NSCE and cluster agreement. The trade-offs between the two objectives for the calibration dataset (2003–2004) consist of 1,150 solutions (gray crosses) obtained from 10 independent NSGA-II runs (Figure 6). The solution where at least one objective value is superior to all other solutions is called the non-dominated solution. In this example, the circles (Figure 6) symbolize a set of non-dominated solution, with 1-NSCE values between 0.16 and 0.29 and agree values between −0.72 and −0.82. Since both the objective functions were used in the minimization problem, the lower

the values of these objectives, the better are the fits of these two objectives. The agree values of −0.72 to −0.82 percentage points indicate that the Pareto solution has a good match with the cluster characterization rules.

The 1-NSCE (∼0.16) values in the Pareto front are similar for the agree values between −0.72 and −0.76 (Figure 6). The 1-NSCE values increase from 0.16 to 0.26 (decrease in NSCE value from 0.84 to 0.74) when the agree values change from −0.76 to −0.78. The 1-NSCE values are greater (NSCE values are lesser) for agree values of −0.80 and −0.82. Based on such results, the solution with the agree value of −0.76 and 1-NSCE value of 0.16 was chosen as a preferred solution (from the Pareto front). The parameter values for the preferred solution are given in Table 2.

Since the cluster results are related to the different flow components, they affect the parameters controlling each component of the hydrograph. In general, since the model is calibrated with interflow ($SH_{max} > 0$), cluster 1 mainly affects the baseflow, which is controlled by m and T_{cor} parameters. Clusters 2 and 5 are related to the dynamic subsurface flow (interflow) region, which is mainly controlled by the SH_{max}, k_H, P_{thres}, r_k, and K_{cor} parameters. Clusters 3 and 4 are related to surface runoff, which is mainly controlled by k_D and c_{melt}. In addition to the horizontal flow components, these parameters also control the vertical movement of water (e.g., percolation and capillary rise). Therefore, the runoff components and the controlling parameters are highly interdependent, and it is not possible to tease out the effects of the individual clusters on the calibrated parameters.

Figure 7(a) and 7(b) show the clusters retrained for daily discharge and nitrate-N datasets for 2003–2004 and 2001 periods, respectively. Due to differences in the temporal resolution, daily clusters are slightly different from hourly clusters. Notably, some of the sub-daily variations are lost due to aggregation to a daily time step (compare Figures 5(a) to 7(a) and 5(b) to 7(b)). However, general patterns in the clusters (in terms of average cluster class values) at corresponding time periods are similar for both time steps.

The discharge hydrograph for the preferred solution, observations, and the cluster classes for the calibration (2003–2004) and validation (2001) datasets are shown in Figure 7(a) and 7(b), respectively. The results show good representation (rising and the recession limbs of the
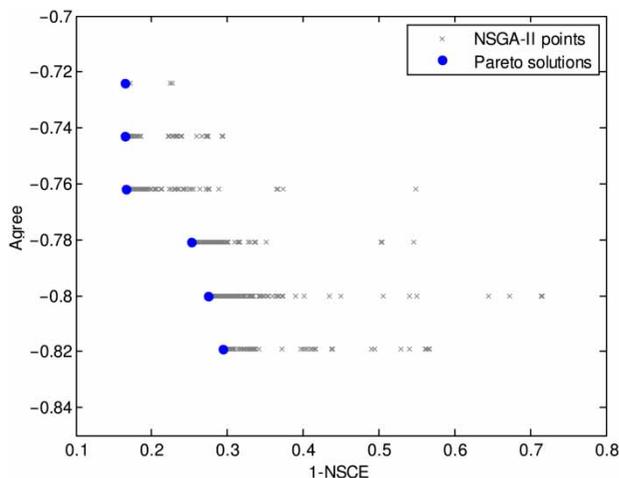

Figure 6 │ Trade off between 1-NSCE and agreement with cluster results (agree).
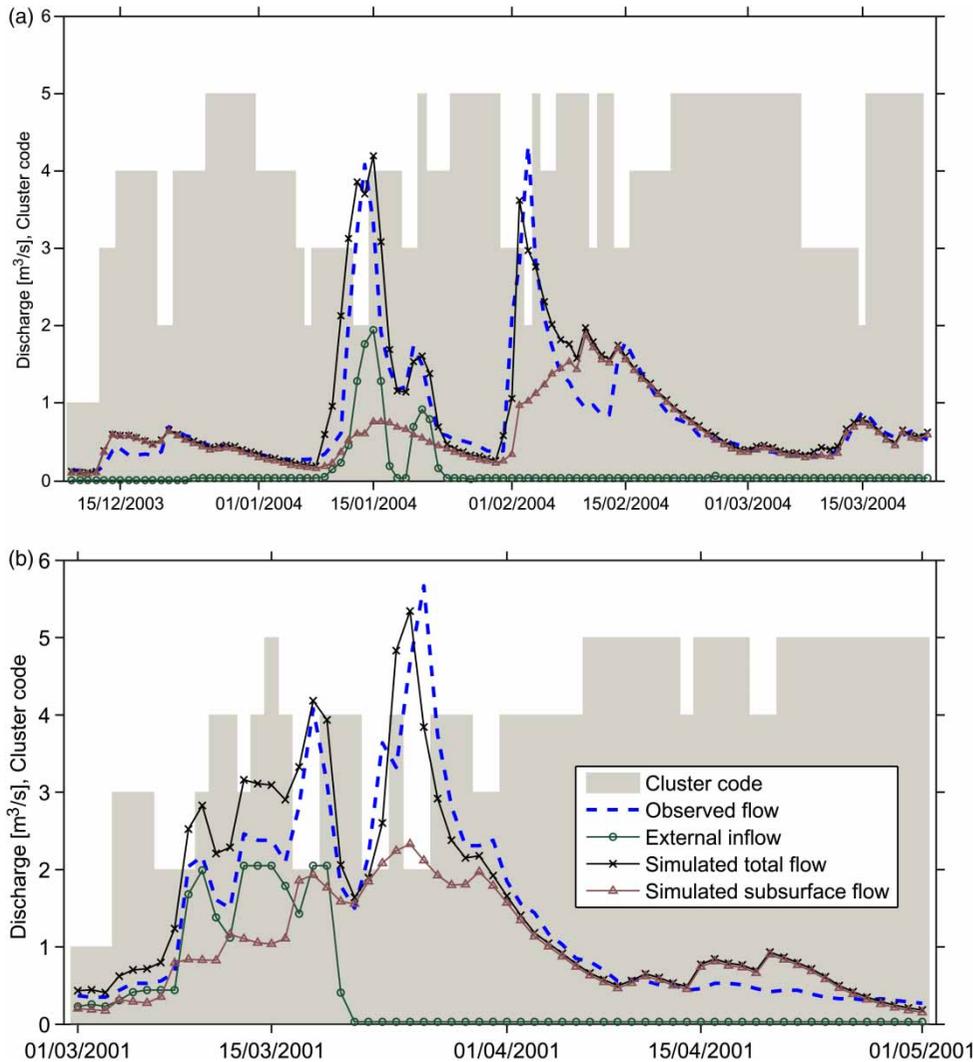
Figure 7 │ WaSiM-ETH model results in comparison to observations and daily discharge–nitrate-N cluster results for: (a) calibration dataset (2003–2004) and (b) validation dataset (2001).

hydrographs as well as low flows) of runoff dynamics of the calibration and validation datasets. The statistical performance of the preferred solution (Table 3) also indicates a good match of the WaSiM-ETH simulation with

Table 3 │ Statistical performance of preferred solution obtained from the WaSiM-ETH calibration

Datasets	Year	Period	NSCE	R^2	MAE [m³/s]
Calibration	2003–2004	Dec. 9–March 23	0.84	0.85	0.21
Validation	2001	March 1–May 1	0.82	0.83	0.34

observations, with slightly better 'goodness of fit' values (NSCE, R^2, and MAE) for the calibration results in comparison to validation results. There are a number of problems in model simulations, such as overprediction and phase shifts of 25/03/2001 and 2/2/2004 peaks, which may be due to uncertainties in the data and model. Overall, the results show the use of discharge–nitrate concentration clusters as soft data in a multi-objective optimization framework helps in choosing a parameter set with reasonable simulation of total runoff, as well as flow components. Although the external inflow complicated the flow separation in this particular case, the hydrological flow

components show a reasonable dynamics of subsurface flow and surface runoff components (Figure 7(a) and 7(b)). Such findings are similar to a study by Seibert & McDonnell (2002), who also found that the use of soft data for calibration helps in choosing the model parameters with good representation of runoff, as well as catchment processes as represented by soft data. Therefore, it can be concluded that the inclusion of soft data also gives modelers increased confidence as it provides a means to indirectly validate the simulated flow components.

The unavailability of sub-daily meteorological inputs is the main limitation in the hydrological model calibration. Hourly calibration of the hydrological model would allow the consideration of sub-daily variations of flow components and their relationships with nitrate response. The sub-daily variations may be especially important to correctly simulate rapid flow components like infiltration excess overland flow or runoff from paved areas. Therefore, calibration of the hydrological model at an hourly time step (with hourly cluster results as soft data) would be a better utilization of high-frequency nitrate data. In principle, the methodology in this study (hydrological model calibration using nitrate-N concentration as soft data) is independent of temporal resolution and could be adapted to a sub-daily time step.

CONCLUSIONS

The study presented a methodology for employing high-frequency discharge–nitrate concentration data for characterizing qualitative flowpaths in a catchment and using the qualitative flowpaths for hydrological model calibration. The nitrate concentration–discharge data are characterized by 'concentration' and 'dilution' patterns with nitrate-N concentration peaks lagging the discharge peaks followed by rapid decline in the concentration as the streamflow hydrograph recedes. Furthermore, nitrate stable isotope ($\delta^{15}N$ and $\delta^{18}O$) data from the catchment indicated low denitrification. Based on these observations, it was considered suitable to employ discharge–nitrate concentration relationship to qualitatively describe the hydrologic flowpaths.

A SOFM-based cluster identification methodology was employed to characterize the flowpaths. The SOFM clusters captured distinctive patterns in the data series, characterized by increase or decrease of nitrate-N concentration corresponding to increase or recession of discharge hydrograph. Based on these distinctive patterns, the identified clusters were characterized using the prevailing understanding of the catchment-scale nitrate response and previous studies of the catchment. Accordingly, five different qualitative patterns in the datasets were identified and conceptually characterized into qualitative flow responses: (1) baseflow; (2) subsurface flow increase; (3) surface runoff increase; (4) surface runoff recession; and (5) subsurface flow decrease regions. The qualitative flow response was employed in an indirect methodology (as soft data) to calibrate the responses simulated by the hydrological model (WaSiM-ETH), where agreement of the simulated flow components with qualitative flowpaths was considered as an objective function. The methodology led to a good agreement of the simulated outputs with the discharge hydrograph as well as qualitative flowpaths. Therefore, the methodology provides increased confidence to the hydrologic model simulations.

The results of the study also showed the potential for employing high-frequency nitrate-N data for understanding qualitative hydrological response and using qualitative flow responses for calibration of a hydrological model. The methodology is restricted to catchments with limited biogeochemical transformation of nitrate (which was found to be the case in the Weida catchment by additional nitrate stable isotope analysis). If considerable denitrification in the subsurface flow or in the streamflow is present, it may not be possible to use nitrate concentrations to directly characterize hydrological response. Another limitation of this study is the unavailability of the sub-daily meteorological inputs, which restricted calibrating the hydrological model, and considering flow components to a daily resolution. In principle, the introduced methodology is independent of temporal resolution and can be employed (with qualitative flow components as soft data) for the calibration of a hydrological model at a sub-daily time step.

ACKNOWLEDGEMENT

REFERENCES

Alexander, R. B., Böhlke, J. K., Boyer, E. W., David, M. B., Harvey, J. W., Mulholland, P. J., Seitzinger, S. P., Tobias, C. R., Tonitto, C. & Wollheim, W. M. 2009 Dynamic modeling of nitrogen losses in river networks unravels the coupled effects of hydrological and biogeochemical processes. *Biogeochemistry* **93**, 91–116.

Alvarez-Guerra, M., González-Piñuela, C., Andrés, A., Galán, B. & Viguri, J. R. 2008 Assessment of Self-Organizing Map artificial neural networks for the classification of sediment quality. *Environ. Int.* **34**, 782–790.

Anderton, S., Latron, J., White, S. M. & Gallart, F. 2002 Sensitivity analysis and multiresponse, multi-criteria evaluation of a physically based distributed model. *Hydrol. Process.* **16**, 333–353.

Arnold, J. G., Allen, P. M., Muttiah, R. & Bernhardt, G. 1995 Automated base flow separation and recession analysis techniques. *Ground Water* **33**, 1010–1018.

ASCE Task Committee on application of Artificial Neural Networks in Hydrology 2000a Artificial neural networks in hydrology. I: Preliminary concepts. *J. Hydrol. Eng.-ASCE* **5** (2), 115–123.

ASCE Task Committee on application of Artificial Neural Networks in Hydrology 2000b Artificial neural networks in hydrology. II: Hydrologic applications. *J. Hydrol. Eng.-ASCE* **5** (2), 124–137.

Bergström, S., Lindström, G. & Pettersson, A. 2002 Multi-variable parameter estimation to increase confidence in hydrological modelling. *Hydrol. Process.* **16**, 413–421.

Beven, K. & Freer, J. 2001 Equifinality, data assimilation, and data uncertainty estimation in mechanistic modelling of complex environmental systems using the GLUE methodology. *J. Hydrol.* **249**, 11–29.

Beven, K. J. & Kirkby, M. J. 1979 A physically based variable contributing area model of basin hydrology. *Hydrol. Sci. Bull.* **24** (1), 43–69.

Bongartz, K. 2004 *Abschlußbericht der FSU Jena zum Forschungsprojekt 'Integriertes Flussgebietsmanagement am Beispiel der Saale' (in German)*. Institut für Geographie, Friedrich-Schiller-Universität Jena, Germany.

Buda, A. R. & DeWalle, D. R. 2009 Dynamics of stream nitrate sources and flowpathways during stormflows on urban, forest and agricultural watersheds in central Pennsylvania, USA. *Hydrol. Process.* **23**, 3292–3305.

Casciotti, K. L., Sigman, D. M., Galanter Hastings, M., Böhlke, J. K. & Hilkert, A. 2002 Measurement of the oxygen isotopic composition of nitrate in seawater and freshwater using the denitrifier method. *Analyt. Chem.* **74**, 4905–4912.

Creed, I. F. & Band, L. E. 1998 Export of nitrogen from catchments within a temperate forest: evidence for a unifying mechanism regulated by variable source area dynamics. *Water Resour. Res.* **34** (11), 3079–3093.

Creed, I. F., Band, L. E., Foster, N. W., Morrison, I. K., Nicolson, J. A., Semkin, R. S. & Jeffries, D. S. 1996 Regulation of nitrate-N release from temperate forests. A test of the N flushing hypothesis. *Water Resour. Res.* **32**, 3337–3354.

Deb, K., Pratap, A., Agarwal, S. & Meyarivan, T. 2002 A fast and elitist multiobjective genetic algorithm: NSGA-II. *IEEE Trans. Evolut. Comput.* **6** (2), 188–197.

Demuth, H., Beale, M. & Hagan, M. 2009 *Neural Network Toolbox 6 User's Guide*, The MathWorks Inc., Online documentation available at: http://www.mathworks.com/access/helpdesk/help/toolbox/nnet/ (August 5 2008).

Eckhardt, K. 2005 How to construct recursive digital filters for baseflow separation. *Hydrol. Process.* **19**, 507–515.

Fink, M. 2004 Regionale Modellierung der Wasser- und Stickstoffdynamik als Entscheidungsunterstützung für die Reduktion des N-Eintrags am Beispiel des Trinkwassertalsperrensystems Weida- Zeulenroda, Thüringen. Dissertation (in German), Jena Friedrich-Schiller-Universität, Chemisch-Geowissenschaftliche Fakultät, Jena, Germany.

Furey, P. R. & Gupta, V. K. 2001 A physically based filter for separating base flow from streamflow time series. *Water Resour. Res.* **37** (11), 2709–2722.

Green, C. T., Böhlke, J. K., Bekins, B. A. & Phillips, S. P. 2010 Mixing effects on apparent reaction rates and isotope fractionation during denitrification in a heterogeneous aquifer. *Water Resour. Res.* **46** (8), W08525.

Hesser, F. B., Franko, U. & Rode, M. 2010 Spatially distributed lateral nitrate transport at the catchment scale. *J. Environ. Qual.* **39**, 193–203.

Hill, A. R. 1979 Denitrification in the nitrogen budget of a river ecosystem. *Nature* **281**, 291–292.

Hong, Y.-S. & Rosen, M. R. 2001 Intelligent characterisation and diagnosis of groundwater quality in an urban fractured-rock aquifer using an artificial neural network. *Urban Water* **3**, 193–204.

Hornberger, G., Bencala, K. & McKnight, D. 1994 Hydrological controls on dissolved organic carbon during snow melt in the Snake River near Montezuma, Colorado. *Biogeochemistry* **25**, 147–165.

Inamdar, S. P., Christopher, S. & Mitchell, M. J. 2004 Flushing of DOC and nitrate from a forested catchment: role of hydrologic flowpaths and water sources. *Hydrol. Process.* **18** (14), 2651–2661.

Jain, A. & Srinivasulu, S. 2006 Integrated approach to model decomposed flow hydrograph using artificial neural network and conceptual techniques. *J. Hydrol.* **317**, 291–306.

Kalteh, A. M., Hjorth, P. & Berndtsson, R. 2008 Review of the self-organizing map (SOM) approach in water resources: analysis, modelling and application. *Environ. Modell. Softw.* **23**, 835–845.

Kendall, C. & Aravena, R. 2000 Nitrate isotopes in groundwater systems. In: *Environmental Tracers in Subsurface Hydrology* (P. G. Cook & A. L. Herczeg, eds). Springer, New York, pp. 261–298.

Kendall, C. & McDonnell, J. J. 1998 *Isotope Tracers in Catchment Hydrology*. Elsevier, Amsterdam.

Kirchner, J. W., Feng, X., Neal, C. & Robson, A. J. 2004 The fine structure of water-quality dynamics: the (high-frequency) wave of the future. *Hydrol. Process.* **18** (7), 1353–1359.

Knöller, K., Vogt, C., Haupt, M., Feisthauer, S. & Richnow, H. H. 2011 Experimental investigation of nitrogen and oxygen isotope fractionation in nitrate and nitrite during denitrification. *Biogeochemistry* **103** (1–3), 371–384.

Kohonen, T. 1990 The Self-Organizing Map. *Proc. IEEE* **78** (9), 1464–1480.

Kohonen, T. 2001 *Self-Organizing Maps, 3rd edn, Springer Series in Information Sciences Vol. 30*. Springer, Berlin.

Kohonen, T., Oja, E., Simula, O., Visa, A. & Kangas, J. 1996 Engineering applications of the self-organizing map. *Proc. IEEE* **84** (10), 1358–1384.

Lin, G.-F. & Wu, M. C. 2007 A SOM-based approach to estimating design hyetographs of ungauged sites. *J. Hydrol.* **339**, 216–226.

Lindenschmidt, K. E., Ollesch, G. & Rode, M. 2004 Physically-based hydrological modelling for nonpoint dissolved phosphorus transport in small and medium-sized river basins. *Hydrol. Sci. J.* **49** (3), 495–510.

Mariotti, A., Germon, J. C., Hubert, P., Kaiser, P., Letolle, R., Tardieux, A. & Tardieux, P. 1981 Experimental determination of nitrogen kinetic isotope fractionation: some principles, principles, illustration for the denitrification and nitrification processes. *Plant Soil* **62**, 413–430.

McHale, M. R., McDonnell, J. J., Mitchell, M. J. & Cirmo, C. P. 2002 A field-based study of soil water and groundwater nitrate release in an Adirondack forested watershed. *Water Resour. Res.* **38**, 1031–1047.

Mulholland, P. J., Helton, A. M., Poole, G. C., Hall, R. O., Hamilton, S. K., Peterson, B. J., Tank, J. L., Ashkenas, L. R., Cooper, L. W., Dahm, C. N., Dodds, W. K., Findlay, S. E., Gregory, S. V., Grimm, N. B., Johnson, S. L., McDowell, W. H., Meyer, J. L., Valett, H. M., Webster, J. R., Arango, C. P., Beaulieu, J. J., Bernot, M. J., Burgin, A. J., Crenshaw, C. L., Johnson, L. T., Niederlehner, B. R., O'Brien, J. M., Potter, J. D., Sheibley, R. W., Sobota, D. J. & Thomas, S. M. 2008 Stream denitrification across biomes and its response to anthropogenic nitrate loading. *Nature* **452** (7184), 202–204.

Ocampo, C. J., Oldham, C. E. & Sivapalan, M. 2006a Nitrate attenuation in agricultural catchments: shifting balances between transport and reaction. *Water Resour. Res.* **42**, W01408.

Ocampo, C. J., Oldham, C. E., Sivapalan, M. & Turner, V. J. 2006b Hydrological versus biogeochemical controls on catchment nitrate export: a test of the flushing mechanism. *Hydrol. Process.* **20**, 4269–4286.

Peter, M. 1988 Zum Einfluss der Abflusskomponenten Q0, QI und QG auf den Stofftransport von Wasserläufen aus Einzugsgebieten verschiedener Bodennutzung in Mittelgebirgen mit speziellen hydromorphologischen Verhältnissen. PhD Thesis, Faculty of Agricultural Sciences, Justus-Liebig University of Giessen, Germany.

Petry, J., Soulsby, C., Malcolm, I. A. & Youngson, A. F. 2002 Hydrological controls on nutrient concentrations and fluxes in agricultural catchments. *Sci. Total Environ.* **294**, 95–110.

Poor, C. J. & McDonnell, J. J. 2007 The effects of landuse on stream nitrate dynamics. *J. Hydrol.* **332**, 54–68.

Rode, M. & Lindenschmidt, K. E. 2001 Distributed sediment and phosphorus transport modelling on a medium sized catchment in central Germany. *Phys. Chem. Earth (B)* **26** (7–8), 635–640.

Rode, M., Thiel, E., Franko, U., Wenk, G. & Hesser, F. 2009 Impact of selected agricultural management options on the reduction of nitrogen loads in three representative meso scale catchments in Central Germany. *Sci. Total Environ.* **407**, 3459–3472.

Royer, T. V., Tank, J. L. & David, M. B. 2004 Transport and fate of nitrate in headwater agricultural streams in Illinois. *J. Environ. Qual.* **33**, 1296–1304.

Rusjan, S., Brilly, M. & Mikos, M. 2008 Flushing of nitrate from a forested watershed: an insight into hydrological nitrate mobilization mechanisms through seasonal high-frequency stream nitrate dynamics. *J. Hydrol.* **354** (1–4), 187–202.

Salvia-Castellvi, M., Iffly, J. F., Borght, P. V. & Hoffman, L. 2005 Dissolved and particulate nutrient export from rural catchments: a case study from Luxembourg. *Sci. Total Environ.* **344**, 51–65.

Savard, M. M., Somers, G., Smirnoff, A., Paradis, D., van Bochove, E. & Liao, S. 2010 Nitrate isotopes unveil distinct seasonal N-sources and the critical role of crop residues in groundwater contamination. *J. Hydrol.* **381**, 134–141.

Schulla, J. 1997 Hydrologische Modellierung von Flussgebieten zur Abschätzung der Folgen von Klimaänderungen. Dissertation (in German), ETH-Zurich, Switzerland.

Schulla, J. & Jasper, K. 2007 Model Description WaSiM-ETH. Technical report, pp. 181. Available at: http://www.wasim.ch/downloads/doku/wasim/wasim_2007_en.pdf.

Seibert, J. & McDonnell, J. J. 2002 On the dialog between experimentalist and modeler in catchment hydrology: use of soft data for multicriteria model calibration. *Water Resour. Res.* **38** (11), 1241, 23-11-23-14.

Sebilo, M., Billen, G., Grably, M. & Mariotti, A. 2003 Isotopic composition of nitrate-nitrogen as a marker of riparian and benthic denitrification at the scale of the whole Seine River system. *Biogeochemistry* **63**, 35–51.

Shomar, B., Osenbrück, K. & Yahya, A. 2008 Elevated nitrate levels in the groundwater of the Gaza Strip: distribution and sources. *Sci. Total Environ.* **398**, 164–174.

Shrestha, R. R. & Rode, M. 2008 Multi-objective calibration and fuzzy preference selection of a distributed hydrological model. *Environ. Modell. Softw.* **239** (12), 1384–1395.

Shrestha, R. R., Bárdossy, A. & Rode, M. 2007 A hybrid deterministic-fuzzy rule based model for catchment scale nitrate dynamics. *J. Hydrol.* **342**, 143–156.

Sigman, D. M., Casciotti, K. L., Andreani, M., Barford, C., Galanter, M. & Böhlke, J. K. 2001 A bacterial method for the nitrogen isotopic analysis of nitrate in seawater and freshwater. *Analyt. Chem.* **73**, 4145–4153.

Soulsby, C., Tetzlaff, D., van den Bedem, N., Malcolm, I. A., Bacon, P. J. & Youngson, A. F. 2007 Inferring groundwater

influences on streamwater in montane catchments from hydrochemical surveys of springs and streamwaters. *J. Hydrol.* **333** (2–4), 199–213.

Spongberg, M. E. 2000 Spectral analysis of base flow separation with digital filters. *Water Resour. Res.* **36** (3), 745–752.

Stieglitz, M., Shaman, J., McNamara, J., Engel, V., Shanley, J. & Kling, G. W. 2003 An approach to understanding hydrologic connectivity on the hill slope and the implications for nutrient transport. *Glob. Biogeochem. Cy.* **17** (4), 1105. 16-1-16-15.

Thüringen State Land Surveying Office 2003 Digitale Geländemodelle (DGM). Available at: http://www.thueringen.de/de/vermessung/.

Van Herpe, Y. J. P. & Troch, P. A. 2000 Spatial and temporal variations in surface water nitrate concentrations in a mixed landuse catchment under humid temperate climatic conditions. *Hydrol. Process.* **14** (14), 2439–2455.

Vanni, M. J., Renwick, W. H., Headworth, J. L., Auch, J. D. & Schaus, M. H. 2001 Dissolved and particulate nutrient flux from three adjacent agricultural watersheds: a five-year study. *Biogeochemistry* **54**, 85–114.

Webb, B. W. & Walling, D. E. 1985 Nitrate behaviour in streamflow from a grassland catchment in Devon, UK. *Water Res.* **19**, 1005–1016.

Xue, D., Botte, J., De Baets, B., Accoe, F., Nestler, A., Taylor, P., Van Cleemput, O., Berglund, M. & Boeckx, P. 2009 Present limitations and future prospects of stable isotope methods for nitrate source identification in surface- and groundwater. *Water Res.* **43**, 1159–1170.